Title
Process-based expansion and neural differentiation of human pluripotent stem cells for transplantation and disease modeling

Journal
Journal of Neuroscience Research, 91(10)

ISSN
0360-4012

Authors
Stover, Alexander E
Brick, David J
Nethercott, Hubert E
et al.

Publication Date
2013-10-01

DOI
10.1002/jnr.23245

Peer reviewed

Published in final edited form as:
J Neurosci Res. 2013 October ; 91(10): 1247–1262. doi:10.1002/jnr.23245.

Process-Based Expansion and Neural Differentiation of Human Pluripotent Stem Cells for Transplantation and Disease Modeling

Alexander E. Stover[1], **David J. Brick**[1], **Hubert E. Nethercott**[1], **Maria G. Banuelos**[1], **Lei Sun**[2], **Diane K. O'Dowd**[2], and **Philip H. Schwartz**[1,*]

[1]National Human Neural Stem Cell Resource, Centers for Neuroscience and Translational Research, Children's Hospital of Orange County Research Institute, Orange, California

[2]Department of Developmental and Cell Biology, University of California, Irvine, Irvine, California

Abstract

Robust strategies for developing patient-specific, human, induced pluripotent stem cell (iPSC)-based therapies of the brain require an ability to derive large numbers of highly defined neural cells. Recent progress in iPSC culture techniques includes partial-to-complete elimination of feeder layers, use of defined media, and single-cell passaging. However, these techniques still require embryoid body formation or coculture for differentiation into neural stem cells (NSCs). In addition, none of the published methodologies has employed all of the advances in a single culture system. Here we describe a reliable method for long-term, single-cell passaging of PSCs using a feeder-free, defined culture system that produces confluent, adherent PSCs that can be differentiated into NSCs. To provide a basis for robust quality control, we have devised a system of cellular nomenclature that describes an accurate genotype and phenotype of the cells at specific stages in the process. We demonstrate that this protocol allows for the efficient, large-scale, cGMP-compliant production of transplantable NSCs from all lines tested. We also show that NSCs generated from iPSCs produced with the process described are capable of forming both glia defined by their expression of S100β and neurons that fire repetitive action potentials.

Keywords

cGMP; cellular therapy; differentiation; cellular models of disease; iPSCs; drug discovery; neural stem cells; neurons; glia; nomenclature; methods

Neurological disorders are a heterogeneous spectrum of diseases and injuries characterized by severe and sometimes progressive cognitive, sensory, and motor deficits. These disorders constitute a large portion of the global burden of disease, estimated at 6.3% by the WHO. In comparison, HIV/AIDS and malignant neoplasms each constitute slightly over 5% of the

*Correspondence to: Philip H. Schwartz, PhD, National Human Neural Stem Cell Resource, Children's Hospital of Orange County Research Institute, 1201 West La Veta Avenue, Orange, CA 92868-4203. pschwartz@choc.org.

Additional Supporting Information may be found in the online version of this article.

total burden. Many neurological diseases lead to death of regional subpopulations of neurons, such as the loss of cholinergic neurons in Alzheimer's disease and γ-aminobutyric acid (GABA)-ergic neurons in Batten's disease (Schwartz et al., 2008). Neurological disease can also be associated with the loss or dysfunction of specific classes of glial cells as occurs in Alexander's disease and in some forms of amyotrophic lateral sclerosis (Schwartz et al., 2008).

Recent advances in stem cell biology and the advent of somatic cell reprogramming technology now allow the generation of patient-specific stem cells that can be differentiated in vitro into a variety of cell types of the nervous system (Takahashi et al., 2007; Yu et al., 2007). These technologies have the potential to develop patient-specific therapies through generation of immune-matched neural cells. Furthermore, they can be useful as in vitro models that facilitate exploration of disease mechanisms, identification of novel therapeutic targets, and diagnostic accuracy. For these applications to be truly successful, however, it is first necessary to devise protocols that allow generation of large numbers of specific cell types for transplantation or disease modeling.

Differentiation of pluripotent stem cells (PSCs) into cells of the neural lineage, therefore, has become a central focus of a number of laboratories and has resulted in the description of several dozen methods for differentiation of neural cells from PSCs (for review see Schwartz et al., 2008). Among these are methods for the generation of neural stem cells (NSCs), dopaminergic neurons, retinal neurons, ventral motoneurons, and oligodendroglial progenitors. Most of the published reports of PSC culture and subsequent neural differentiation describe a sequence of steps that generally includes coculture with feeder cells (or use of feeder cell-conditioned medium), serum-based media, manual passaging (or passaging of the cells as clumps of cells), manual picking of undifferentiated or differentiated cell clusters to maintain culture integrity, alternation between adherent and nonadherent culture, and often subjective cell purification methods.

Use of these methodologies has led to the production of at least one FDA-approved transplantable neural cell product using ePSCs (embryo-derived pluripotent stem cells) as the starting material. However, the extensive characterization needed for the end product, the transplantable cells, precludes their general application to patient-specific therapies. In addition, this type of approach is completely dependent on concomitant immunosuppressive therapies, because HLA matching is virtually impossible.

A truly patient-specific approach has at its core two basic components: use of identified cell subtypes specifically targeted to the disease process needing treatment and an HLA-matching strategy that eliminates the need for aggressive or long-lasting immunosuppression. To increase the success of patient-specific therapies based on iPSC technologies, it is important to develop well-defined production methods in which the production process is characterized in great detail. Such a "process-based" approach will facilitate use of these cells for transplantation in a patient-specific manner. In addition, a process-based approach will also be critical in disease-modeling applications, in which it is important that differences observed between diseased cells and normal cells are related to the disease and not the method used to derive the cells (Belmonte et al., 2009).

Here we describe a method that combines and extends advances in PSC derivation and culture and subsequent neural differentiation into a single, reproducible cell culture method. We also describe a nomenclature to accurately distinguish the genotype and phenotype of the cells at specific points along the process and allow qualification criteria to be applied at critical junctures. This process-based production of PSC-derived neural cells is suitable for transplantation or disease modeling. The process, while aimed primarily at producing NSCs, is validated insofar as it has been shown to be successful with all four ePSC and seven iPSC lines studied. With one of the iPSC lines, we have repeatedly demonstrated that the resulting NSCs are capable of maturing into neurons that fire repetitive action potentials or glial cells that are defined by their expression of S100β.

MATERIALS AND METHODS

Supporting Information

Many of the Materials and Methods are described in the Supporting Information, because they have been reported elsewhere but have particular nuances included. Notably, included in the Supporting Information is our system of nomenclature (Supp. Info. Table I) that is useful for keeping track of each of the many different cellular phenotypes produced.

Cell Lines

ePSCs—The following human ePSCs, each listed on the NIH Human Embryonic Stem Cell Registry at the time when the experiments were performed using particular NIH funds, were obtained from commercial sources: WA01.1-EI25 (H1, male karyotype; WiCell, Madison, WI), WA09.1-EI26 (H9, female karyotype; WiCell), BG01.1-EI26 (hESBGN.01, male karyotype; Bresagen, Athens, GA), and BG03.1-EI27 (hESBGN.03, female karyotype; Bresagen).

Somatic cells—Skin biopsies from fragile X syndrome (FXS) and autism spectrum disorder (ASD) patients and normal controls (SC101.7-S, SC103.5-S, SC105.9-S, SC110.4-S, SC122.6-S, SC151.7-S, and SC171.7-S) and normal (SC30.1-BN15) brain-derived NSCs (Schwartz et al., 2003) were obtained under IRB-approved protocols, either at CHOC or UC Davis. Explant fibroblast cultures (SC101.7-SF4, etc.; see Supporting Information) were established from the skin biopsies in D-MEM, high-glucose, with GlutaMax, 10% fetal bovine serum (FBS), 1× nonessential amino acids (NEAA), 10 μM Primocin (Invivogen, Carlsbad, CA) after finely mincing the tissue with scalpel blades. These cultures were passaged three or four times with Tryple Express (Life Technologies, Grand Island, NY; 12604) before banking, distribution, or use. Lentivirus transduction of fibroblasts to iPSCs is described in the Supporting Information.

Hematopoietic stem cells (HSCs)—The isolation of human umbilical cord blood HSCs is described in the Supporting Information.

Lentivirus Preparation and Derivation of iPSC Lines From Fibroblasts

The production of iPSCs from fibroblasts by lentivirus transduction is described in the Supporting Information.

Sendai Virus Derivation of iPSC Lines From HSCs and Fibroblasts

Primary $CD34^+$ HSCs (7×10^5 HSCs were derived from fresh human umbilical cord blood as described in the Supporting Information) and seeded in one well of a six-well tissue-culture-treated plate and cultured in 4 ml $CD34^+$ culture medium (Kambal et al., 2011): Iscove's modified Dulbecco's medium (IMDM; Life Technologies), supplemented with 1:100 GlutaMax, 10% FBS (Atlanta Biologicals, Atlanta, GA; S11550), 50 ng/ml TPO (Peprotech, Fair Lawn, NJ; 300-18), 50 ng/ml SCF (Peprotech; 300-07), and 50 ng/ml Flt3 (Peprotech; 300-19). Medium was exchanged 100% every other day for a maximum of 4 days before reprogramming.

Cultured $CD34^+$ HSCs (1×10^5) were seeded in one well of a 12-well tissue-culture-treated plate in 0.5 ml $CD34^+$ culture medium. $CD34^+$ HSCs were reprogrammed using the CytoTune Sendai Reprogramming Kit (Life Technologies; A1377801), by directly adding the individual transgene-containing viruses (OCT3/4, SOX2, KLF4, c-MYC) to the well at a multiplicity of infection (MOI) of 3. The plate was rocked every 30 min for 2 hr. After 24 hr, transduced $CD34^+$ cells were centrifuged at 200*g* for 5 min. The pellet was resuspended in $CD34^+$ culture medium and cocultured in one six-well plate, prepared with irradiated ICR mouse embryonic fibroblasts (MEFs; 2×10^4 cells/cm^2; Life Technologies; S1520-100). On the next day, the medium was collected and centrifuged at 200*g* for 5 min. The pellet was resuspended with 100% traditional hESC culture medium (see below), reseeding in the same six-well plate. Medium was exchanged by this method daily for 1 week. After 1 week, medium was exchanged daily, without centrifugation of the removed medium.

Clonal colonies with PSC morphology that stained strongly positive for Tra-1–60 (and some negative for Hoechst, iPSC colonies), were picked for expansion between days 14 and 20 posttransduction. Ten colonies from each HSC line (designated, for example, SC53.1-UH1–2Ix, where x equals 1–10) were initially expanded for at least two passages, and then the three colonies that showed the best morphology and homogeneity of staining with the PSC markers, Nanog and Oct-4, were continuously expanded in culture. iPSC cultures were cryopreserved in 45% PSC medium, 45% FBS or KSR, with 10% DMSO, and stored under liquid nitrogen.

PSC Culture, Traditional

All PSCs (ePSCs and iPSCs) were initially cultured using traditional methods (Schwartz et al., 2011). Under these conditions, the cells grow as tightly compact colonies of cells with characteristic high nucleus-to-cytoplasm ratios. The supporting feeder cells were gamma-irradiated (30 Gy), mitotically inactivated, low-passage, CF-1 strain MEFs (Life Technologies). Six-well plates were coated with 0.1% gelatin for 24 hr before plating MEFs in the same medium used to culture human fibroblasts (see above). Twenty-four hours after the MEFs attached, the medium was aspirated, and the MEFs were rinsed with PBS. One milliliter per well of traditional PSC medium (DMEM/F12, 20% KSR by volume, 100 μM β-mercaptoethanol, 4mM L-glutamine, 1:100 NEAA, 20 ng/ml basic fibroblast growth factor [bFGF]) was then added. MEFs were allowed to condition this medium for at least 1 hr before seeding PSCs suspended in traditional PSC medium. Plates were incubated, humidified, at 37°C under 5% CO_2.

For passaging, the culture medium was replaced with fresh PSC medium, and the colonies were dissected, by hand, under a low-power dissecting microscope (in a BSL-2 biosafety cabinet). The cell clumps were gently triturated and then plated into culture dishes prepared with MEF feeder layers.

PSC Culture, Revised

Transitioning to defined medium—Cells cultured using traditional methods were first transitioned for long-term, feeder-free culture (Stover and Schwartz, 2011). Feeder-cell-grown cultures were first fed with a mixture of 1:1 StemPro hESC SFM (Life Technologies; StemPro)/traditional PSC medium daily for 2–3 days prior to passage. The culture was fed with 100% StemPro 24 hr prior to passaging. On the day of passage, the medium was exchanged with fresh StemPro, and the colonies were mechanically passaged onto a fresh Matrigel-coated plate. Cultures were then fed daily with StemPro until the colonies had grown such that an average colony on the plate completely filled a ×10 objective view under the microscope (Olympus CKX41). Some moderate differentiation appeared during this adaptation phase. Differentiated cells and colonies were mechanically removed before proceeding. When the undifferentiated colonies were large enough to be passaged, they were lifted with Accutase (Life Technologies; see below).

Single-cell passaging—After medium aspiration and rinsing with PBS, 1 ml of 37°C Accutase was added to each well (Bajpai et al., 2008). Cultures were then observed carefully, at room temperature, under a phase-contrast microscope, until individual cells detached from the dish. Lifting cells exhibited an increase in phase brightness and a rounded appearance. After 1–2 min, the vast majority of the cells appeared very phase bright and rounded. Accutase was then diluted sixfold by the addition of 5 ml PBS, and the cells were dissociated by gentle trituration. The cell suspension was then transferred to a conical tube, and the wells were rinsed with an additional 5 ml DPBS to harvest any remaining cells, especially around the edges of the well, and to dilute the Accutase further. The cells were spun at 200*g* for 5 min at room temperature and resuspended in 2 ml StemPro. Cells were then plated at a minimum of 4×10^4 to 1×10^5 cells/cm^2 in fresh, Matrigel-coated wells. On average, a given plating yielded approximately six times the number of plated cells by the end of 1 week, so the standard protocol was to passage approximately 1:6 each week (i.e., there was the potential to produce, from an initial plating of 1×10^6 cells in each well of one six-well plate, 2.8×10^{11} cells in 1,296 six-well plates in six passages). To aid recovery of the cells and help prevent aneuploidies (see below), rho-associated protein kinase (ROCK) inhibitor Y27632 (Stemgent, Cambridge, MA; 04–0012; Watanabe et al., 2007) was added to StemPro (at a final concentration of 10 μM) for the plating immediately following Accutase lifting of the cells. Cryopreservation and thawing of these cells as well as methods for genetic modification and karyotyping are described in the Supporting Information.

NSC Differentiation

Adherent single-cell-passaged cultures of PSCs were allowed to reach confluence and then cultured for an additional 24 hr in StemPro (i.e., they were “superconfluent”). The medium was switched to 1:1 StemPro:Noggin-SB medium (Chambers et al., 2009). Noggin-SB medium consisted of DMEM/F12 GlutaMax (Life Technologies), 10% BIT 9500 (Stem Cell

Technologies, Vancouver, British Columbia, Canada; 09500), 10 μM β-mercaptoethanol (Life Technologies; 21985-023), 100–500 ng/ml Noggin (R&D Systems, Minneapolis, MN; 3344-NG; recombinant human Noggin Fc chimera; see below), and 1 μM SB431542 (SB; Sigma; S4317). SB was prepared at 10 mM in DMSO and filter sterilized. After 24 hr, the cells were switched to 100% Noggin/SB medium and fed daily by complete exchange. After 2 weeks, SB was withdrawn from the Noggin/SB medium. One week later, the neural differentiating cultures were switched to a modified growth medium, GM, (Schwartz et al., 2003) consisting of DMEM/F12 GlutaMax (Life Technologies), 10% BIT 9500 (Stem Cell Technologies; 09500), 10 μM heparin (Sigma; H3149), 20 ng/ml FGF (a kind gift of the National Cancer Institute), and 20 ng/ml EGF (R&D Systems; 236-EG). On the next day, the cultures were gently dissociated using Cell Dissociation Buffer (Life Technologies; 13150-016) and split 1:2 onto Matrigel in the same medium. From that point onward, the cells received a half-medium exchange every 2–3 days and were split 1:2 every 14 days, depending on their growth. Characterization for expression of neural and PSC markers was performed between days 21 and 300 after onset of neural differentiation. For comparison with Noggin, the defined chemical DMH1 (Sigma; D8946) was prepared at 2 mM concentration in DMSO and filter sterilized (Hao et al., 2010; Neely et al., 2012). DMH1 and SB were used at final concentrations of 2 μM and 10 nM, respectively. Additionally, ROCK inhibitor enhancement of DMH1/SB neural differentiation experiments was carried out at the time of passage either in the absence or in the presence of the ROCK inhibitor Y27632 (Stemgent; 04–0012) at 10μM.

In Vivo Assessments

In vivo assessment of tumorigenicity and tissue distribution after transplantation of iPSCs and the NSCs derived from them are described in the Supporting Information.

HLA Typing

Total DNA was harvested from approximately 4×10^6 $CD34^+$ HSCs and 2×10^6 $CD34^+$-derived iPSCs (designated SC53.1-UH1 and SC53.1-UH1UH1–2I1.M5S5, respectively) using the DNeasy Blood and Tissue kit (Qiagen, Valencia, CA; No. 69504) according to the manufacturer's instructions, with the following modification: the DNA was eluted from the DNeasy column in a total volume of 60 μl. HLA typing, utilizing the sequence specific primer (SSP) methodology and the sequence-based typing (SBT) technology, was carried out by HLA Lab Services (Brown Deer, WI) from Life Technologies. The following alleles were typed: A, B, C, DRB1, DQA1, DQB1, and DPB1. These collectively account for more than 96% of possible HLA alleles according to the IMGT/HLA database (Robinson et al., 2009).

Immunocytochemistry

PSCs or NSCs were plated onto Matrigel-coated glass chamber slides (Nunc, Roskilde, Denmark), allowed to adhere, and cultured as appropriate for 2–3 days. Cultures were gently washed with PBS prior to fixation with freshly prepared, 4%, neutral-buffered paraformaldehyde for 5 min at RT. Immunocytochemical analyses were carried out without permeabilization for the detection of cell surface markers and with permeabilization (inclusion of 0.3% Triton X-100) for the detection of cytoplasmic or nuclear antigens

(Nethercott et al., 2011). Nonspecific antigen binding sites were blocked using 3% normal donkey serum (Jackson Immunoresearch, West Grove, PA; 017-000-121). Primary antibodies, all utilized at a 1:100 dilution, unless otherwise noted, were Forse-1 (DSHB, Iowa City, IA), N-CAM (Millipore, Bedford, MA; AB5032), N-CAD (Santa Cruz Biotechnology, Santa Cruz, CA; sc-59987), Pax-6 (Covance, Berkeley, CA; PRB-278P), Oct-4 (Santa Cruz Biotechnology; sc-5279), Sox-2 (Santa Cruz Biotechnology; sc-17320), Sox-1 (R&D Systems; AF3369, 1:50), Olig-2 (Santa Cruz Biotechnology; sc-19969), Tbr-2 (Millipore; AB2283), MASH-1 (BD Pharmingen, San Jose, CA; 556604), β-tubulin (Millipore; MAB1637), β-tubulin (Covance; MRB-435P), MAP2ab (Sigma; M 1406), synapsin (Millipore; AB1543), VGLUT1 (Millipore; AB5905), PSD-95 (Life Technologies; 51–6900), and the human cytosolic-specific marker STEM121 (StemCells, Inc., Palo Alto, CA; 1:2,000). Secondary antibodies (DyLight) were all obtained from Jackson Immunoresearch and used at a 1:1,000 dilution. Biocytin-loaded neurons were detected using a streptavidin-AlexaFluor488 conjugate (Life Technologies; S32354; 1:1,000). Slides were mounted using Prolong Gold Antifade reagent with DAPI (Life Technologies; P36935), and immunoreactive cells were visualized with an Olympus IX70 microscope equipped with appropriate excitation and emission filters designed to minimize spectral overlap. Digital images were obtained using an Optronics Macrofire CCD monochromatic camera. Image files were managed with Image Pro Plus 4.0 software and assembled for publication in Adobe Photoshop CS2. False-color images were made only when overlays were needed to illustrate a given point.

Flow Cytometry

Characterization of the cells by flow cytometry is described in the Supporting Information.

Neuronal Differentiation

Bellco glass coverslips were placed in individual wells of a 24-well plate and coated with poly-D-lysine (PDL; 100 μg/ml; Sigma; P7886). Coverslips were incubated overnight at room temperature and then washed three times with sterile water and air dried. To prepare astrocyte-enriched feeder layers, a 100-μl drop of cell suspension prepared from the cortex of a newborn mouse (P0–P2) was plated onto the PDL-coated coverslips. The 24-well plate was placed in a 37°C incubator for 2 hr, and then each well was flooded with MEM. NSCs were plated onto the coverslips at a density of 5×10 cells/cm^2 when the glial cells had reached ~75% confluence. This coculture was transitioned in 1:1 modified GM:neuronal differentiation medium for 1 day. Neuronal differentiation medium was used thereafter and exchanged 50% daily. Neuronal differentiation medium (Brennand et al., 2011) was made fresh daily and consisted of Neurobasal medium (Life Technologies; 21103) supplemented with 1:100 GlutaMax (Life Technologies; 35050), 1:100 B27 (Life Technologies; 17504-044), 1:100 N2 (Life Technologies; 17502-048), 20 ng/ml BDNF (Peprotech, Hawthorne, NJ; 450-02), 20 ng/ml GDNF (Peprotech; 450-10), 1 mM dibutyryl cAMP (Sigma; D0627), and 200 nM freshly made ascorbic acid (Sigma; A-4034). Dibutyryl cAMP was prepared in D-PBS to a concentration of 1 M, or 1,000×, filter sterilized, and stored in small aliquots at −20°C.

Electrophysiology

Whole-cell recordings were made using unpolished glass pipettes with open tip resistances of 5–8 MΩ (Hilgenberg et al., 2002; Schwartz et al., 2003). Evoked action potentials and voltage-gated currents were recorded using an internal solution containing (in mM): potassium gluconate 120, NaCl 20, $CaCl_2$ 0.1, $MgCl_2$ 2, EGTA 1.1, HEPES 10, Na_2ATP 4.5, all at pH 7.2. Biocytin (0.4%) was added to internal solutions to allow labeling of a subset of cells. The external solution contained (in mM): NaCl 120, KCl 5.4, $MgCl_2$ 0.8, $CaCl_2$ 1.8, glucose 15, HEPES 20, all at pH 7.2. All data shown are corrected for the 5-mV liquid junction potentials generated in these solutions. Data were acquired at room temperature with a List EPC7 amplifier, a Digidata 1320A D-A converter (Axon Instruments, Burlingame, CA), and pClamp8 (Axon Instruments) software.

RESULTS

Our overall goal was to develop a technically easy, xeno-free (capable), and scalable process to produce a defined NSC population for transplantation from any starting PSC culture.

Transitioning ePSCs Grown in Traditional Cultures to Single-Cell Passaging in Defined Medium

Under traditional culture conditions, ePSC-derived colonies grow tight and compact, surrounded by their MEF feeder cells (Fig. 1A). After Accutase passaging, the PSCs that attach to the substrate are typically surrounded by large amounts of membranous material (Fig. 1B). Time-lapse videomicrography of the Accutase-passaged cells indicates that the cells rapidly agglomerate after plating. The cells that do not cluster do not survive (Fig. 1C; Supp. Info. Video 1). Similar to classical PSC culture, the cells attain a high nucleus-to-cytoplasm ratio and exhibit prominent nucleoli as they expand. We typically passage cells 1:6 at confluence or near confluence. Accutase-passaged cells can be seeded back at low densities onto an MEF layer in traditional PSC medium, where they again take on classical ePSC colony morphology within 24 hr postplating (data not shown).

Although Accutase-passaged PSCs migrate to form colonies, the number of colonies is reduced in plates with low seeding densities (data not shown). Underseeded plates can eventually recover with time, but cells under these growth conditions display more uncontrolled differentiation and higher rates of apoptosis than plates seeded at high densities. Consistent with previous studies (Watanabe et al., 2007), we found that addition of an ATP-competitive ROCK inhibitor to the *plating* medium at 10 μM enhances cell survival following passage at either low or high density. With our protocol, one confluent well of a six-well plate generates on average $2.6 \pm 0.6. \times 10^6$ cells by 5 days after plating (SD, N = 8) and it is possible to perform routine 1:6 splits every 5–7 days (at a seeding density of 4×10^4 to 1×10^5 cells/cm^2; Fig. 2). There is some variability in the rate of expansion between cell lines, so this rate should be determined for each specific line to facilitate scale up.

We have successfully cultured ePSCs (WA09.1-EI26, BG01.1-EI26, BG03.1-EI27) in StemPro with Accutase passaging for up to 20 passages (a 3×10^{15}-fold expansion just in StemPro, potentially yielding $1–2 \times 10^{21}$ cells from one six-well plate of starting material

with no picking of colonies), without seeing karyotypic abnormalities (Fig. 3A). Addition of the ROCK inhibitor Y-27632 to StemPro at 10 μM at the time of resuspension and plating prevented the appearance of aneuploidies (Fig. 3B) out to at least 40 passages (a 13×10^{30}-fold expansion; data not shown), which is well past the passage number that would be required for cell production applications for research or therapy. Some of the higher-passaged cells (above passage 20 without ROCK inhibitor) did display common PSC trisomies, such as 12 (Fig. 3C) and 17. Therefore, it is still important to karyotype PSCs grown in this as in other culture systems regularly and to keep reserves of earlier passages banked.

Single-Cell-Dissociated PSCs Are Readily Amenable to Genetic Modification

An inherent difficulty in classical ePSC culture has been low efficiencies of the genetic modification. We have found that single-cell Accutase-lifted PSCs are readily transduced (up to 100%) in suspension with green fluorescent protein (GFP)- or mCherry-labeled lentiviruses prior to plating as adherent cultures on Matrigel (Supp. Info. Fig. 1). In addition, the high lentiviral transduction rate overcomes the need to flow-sort the labeled cells after transduction.

iPSC Colony Cultures Transitioned to Single-Cell Passaging in Defined Medium Maintain Immunologic Integrity

iPSCs present unique opportunities for studying development, in vitro disease modeling, and the generation of patient-specific cell types for transplantation. As the iPSCs are autologous to the patient, the need for immunosuppression is reduced or eliminated. To determine whether iPSCs were also amenable to single-cell passaging using Accutase and continuous culture in StemPro, we transduced low-passage, rapidly dividing human fibroblasts from normal, unaffected and autism spectrum disorder individuals (SC101.7-SF4, SC103.5-SF4, SC105.9-SF4, SC110.4-SF4, SC122.6-SF4, SC151.7-SF4, and SC171.7-SF4) with three lentiviruses. The lentiviruses contained the reprogramming transgenes for OCT4 with SOX2, KLF4 with c-MYC, and NANOG with LIN28, respectively. We also used four nonintegrative Sendai virus (SV) vectors that express OCT4, SOX2, KLF4, or c-MYC. These produce transgene-free iPSCs following propagation and passage (the SV genomes and antigens are diluted out and lost within 8–12 passages while maintaining pluripotency of the resulting iPSCs). iPSC colonies were selected and propagated based on morphological similarity to ePSCs on MEFs and live-cell fluorescence immunostaining for the well-established marker of PSCs Tra-1–60 (Fig. 4A–D). Accutase passaging and StemPro expansion gave rise to iPSC colonies that displayed all of the classical markers of pluripotency (Fig. 4E–L). Because our goal was to generate lines capable of producing NSCs, we did not take further steps to ensure absolute pluripotency of the iPSCs generated.

In addition, we have successfully reprogrammed cord-blood-isolated $CD34^+$ HSCs to iPSCs. For the use of iPSCs in transplantation, examination of the most variable HLA loci (A, B, C, DRB1, DQA1, DQB1, and DPB1) utilizing the sequence specific primer (SSP) methodology and the sequence-based typing (SBT) technology revealed no change in any of the alleles at any of the monitored loci (representing >96% of all known alleles) between the starting $CD34^+$ HSC population transduced with Sendai virus and the resulting reprogrammed iPSCs

(Table I). These data suggest that, in addition to maintaining karotypic stability, these culture methods maintain HLA stability, the most important immunologic consideration for transplantation.

Efficient Neural Differentiation of Confluent, Adherent Cultures of PSCs

Elegant studies have identified the bone morphogenetic protein (BMP), transforming growth factor-β (TGF-β), Notch, and Wnt/B-catenin pathways as playing major roles during neural development. We investigated a number of chemical and/or recombinant approaches to identify methodologies resulting in the optimal yield of NSCs from our adherent PSC cultures. BMP and TGF-β inhibition produced cultures that were uniformly Pax-6-positive, Oct-4-negative primitive neuroepithelial cells (Fig. 5A,B) and that contained neural rosettes (Fig. 6A) and eventual NSCs (Fig. 6B,C). The resulting NSCs compared favorably with brain-derived NSCs on morphological grounds (Fig. 6D) as well as immunohistochemical detection of specific antigens (Fig. 5C–J; Supp. Info. Fig. 1; Schwartz et al., 2003).

Combining defined NSC differentiation with chemically defined PSC growth allowed for refinements in the Noggin/SB differentiation protocols described above. The Accutase single-cell-passaged cells were already grown under feeder-free conditions, so the need for a transition step to Matrigel was eliminated. We have found that, by using a simple, base-medium containing DMEM, BIT 9500, and β-mercaptoethanol, the working concentration of Noggin could be substantially reduced from 500 to 100 ng/ml and still produce a culture of nearly 100% Pax-6-positive neuroepithelial cells. This allowed for a significant reduction in the cost of the neural differentiation procedure with this recombinant protein.

Because each human PSC or iPSC clone may exhibit different propensities to undergo neural differentiation, and because this lineage was our sole focus, we investigated the neural differentiation of several cell lines, including ePSCs (WA01.1-EI25-000.M8S10, BG01.1-EI27-000.M6S25, and BG03.1-EI26-000.M2S4) and normal (SC30.1-SF10-1I5.M5S10 and SC171.7-SF5-1I1.M6S10) and ASD-specific (SC101.7-SF4-1I1.M24S3, SC103.5-SF4-1I3.M24S3, and SC105.9-SF4-1I6.M23S9) iPSCs.

We found Noggin/SB-induced neural differentiation, in conjunction with Accutase, single-cell-passaged, StemPro-expanded, adherent cultures, to be reproducible among all ePSC and iPSC cell lines tested, giving rise to NSCs with properties consistent with those previously reported (Schwartz et al., 2003). The procedure requires no selection method and few transition steps. However, the starting culture density was found to be important; using PSC cultures that had attained confluence and then culturing them for an additional 24 hr ensured that the resulting neuroepithelial cultures were p75 negative (a marker for peripheral nervous system stem cells; Supp. Info. Fig. 3).

Dorsomorphin has been reported to promote human ePSC renewal and also to inhibit BMP signaling through selective inhibition of the BMP type 1 receptors ALK-2, ALK-3, and ALK-6 (Gonzalez et al., 2011; Morizane et al., 2011). To test whether DMH1, a dorsomorphin homologue and far more specific inhibitor of BMP, could effectively substitute for Noggin used in many standard neural differentiation protocols, we compared the combination of DMH1 (2μM) and SB (10 nM) in parallel with Noggin (100 ng/ml) and

SB (1 μM) on neural induction of several ePSC cell lines BG01.1-EI27-000.M6S25, and BG03.1-EI26-000.M2S4 and ASD specific-iPSC lines SC105.9-SF4-1I6.M20S12, SC122.6-SF4-1I1.M20S13, and SC123.4-SF4-1I1.M17S10.

We found that DMH1 could effectively substitute for Noggin in our protocols and lead to robust Pax-6 staining and neural rosette formation in all cell lines examined. Elimination of recombinant proteins during differentiation allows for completely defined, small-molecule-mediated neural differentiation. This is critical for the development of clinical-grade, xeno-free NSCs for transplantation. Using both BG01.1-EI27-000.M6S22 and WA09.1-EI26-000.M8S22 cell lines, we also supplemented the neural induction protocol of DMH1 (2 μM) and SB (10 nM) with ROCK inhibitor (Y-2763210μM) at the time of passage. Comparison of the defined, small-molecule neural differentiation with and without ROCK inhibitor clearly showed that ROCK inhibition at the time of passage can further enhance rosette formation and neural induction (data not shown).

Neural cultures derived en masse using these protocols had no detectable Oct-4 (by immunocytochemistry; Fig. 5A) or Tra-1–60 (by flow cytometry; Supp. Info. Fig. 3, right), indicating that few, if any, undifferentiated PSCs remained in the differentiated cultures. This is critical for any protocol that is slated for eventual human transplantation, because undifferentiated cells within a transplant carry an inherent risk of tumor formation. Throughout these neural differentiation studies, Pax-6 expression was found to be a strong and reliable marker of successful neural induction (Fig. 5), as indeed were Forse-1, Sox-1, and Sox-2. Undifferentiated ePSCs and iPSCs were also stained as controls. Unexpectedly, these experiments indicated that Forse-1, Sox-1, N-CAD, and N-CAM could all stain PSCs to varying degrees (Table II). Forse-1 appeared more prominently expressed in iPSCs than ePSCs, but both stained positive for Sox-1, Sox-2, N-CAD, and N-CAM. PSCs also stained positively for nestin (Table II), a classic marker for intermediate filament proteins in NSCs as well as cells of endodermal lineage, and for Tbr-2, a marker of radial glial cells. However, all undifferentiated PSCs universally stained negative for Pax-6 (data not shown), adding further weight to Pax-6 as a critically important and useful cell marker for monitoring the success of neural induction strategies. This is consistent with previous studies that identified Pax-6 as an early indicator of neural lineage fate (Pankratz et al., 2007). Upon single-cell passage and neural differentiation in chemically defined media, cells become strongly N-CAD-, Sox-1-, FORSE-1-, nestin-, CXCR-4-, and Pax-6-positive, with a number of more mature NCAM-positive cells also detected (Fig. 5). At later stages of differentiation (>16 weeks), OLIG-2 and β-tubulin (which are absent in PSCs) became prominent (Fig. 5), consistent with reports on brain-derived NSCs (Schwartz et al., 2003).

Process-Derived NSCs, in Contrast to PSCs, Are Nontumorigenic In Vivo

The potential tumorigenicity of iPSC-derivatives is of great importance to the cellular therapy field. Although a traditional teratoma assay may be used to determine the tumorigenicity of any specific PSC line, it is most commonly used to demonstrate pluripotency. More germane to potential therapeutic applications is the potential tumorigenicity of the actual cells to be transplanted at the site of transplantation. We found, in distinct contradiction to other reports (Muotri et al., 2005), that PSCs injected

intracerebroventricularly (N = 20) consistently gave rise to periventricular intracranial tumors of unknown composition (Fig. 7A,B). It is of interest to note that coinjected GFP- and mCherry-labeled PSCs gave rise to apparently segregated tumors (Fig. 7A,B). Because the cells were thoroughly mixed before injection, this segregation suggests that some of the tumors were clonally derived, implying only some of the cells maintain a tumorigenic potential after injection into the ventricles.

On the other hand there was no evidence of intracranial tumors associated with PSC-derived NSCs derived and cultured according to our methodologies and injected in an identical manner (N = 15; Fig. 7C–H). These cells migrated widely throughout the brain and took up long-term (>15 months) residence in both cortical and subcortical structures. Although many cells had a neuronal appearance, showing putative apical neurites, future studies will be needed to determine the actual phenotypes of these transplanted cells.

Process-Derived NSCs Yield Glia and Functionally Active Neurons In Vitro

To determine whether the SB- and DMH1-induced NSCs were capable of differentiating into mature neurons, we cultured the NSCs derived from one line, SC122.6-SF4-1I1.M7S13-N2G4-2Nn35–70, for >3 and up to 10 weeks with BDNF, GDNF, cAMP, and ascorbic acid in coculture with primary cortical mouse or rat astrocytes (Brennand et al., 2011). This extended differentiation resulted in a large number of cells exhibiting neuronal morphology with numerous long processes and staining strongly positive for βIII-tubulin, synapsin, VGlut, PSD95, and MAP2ab (Fig. 8A,B).

To test the capacity of the process-derived NSCs to form astrocytes, we cultured the DMH1 and SB-induced NSCs as neurospheres in NSC media for 11 weeks. This was followed by treatment with N2 and CNTF for 6 days, gentle mechanical dissociation of the spheres, and plating on Matrigel with with N2, FBS, and EGF for an additional 2 weeks. This differentiation procedure resulted in a highly efficient induction of astrocytes that strongly and uniformly stained for the astrocyte-specific marker S100β (Fig. 8C).

Electrophysiological analysis was performed on cells between 8 and 10 weeks in culture. Cells targeted for whole-cell recordings had a clearly defined somatic region and one or more branched processes. All neurons with input resistances greater than 200 MΩ exhibited composite currents with both an inward sodium and outward potassium component in response to a series of depolarizing voltage steps (n = 68; Fig. 9A). The average peak inward current amplitude was 342.3 ± 48.4 pA. Evaluation of the same cells in current clamp revealed that 14.1% were also electrically excitable, firing action potentials in response to injection of depolarizing current (Fig. 9B). The remainder exhibited only small depolarizing deflections without a clear inflection on the rising phase, responses characteristic of immature neurons.

To confirm that the electrophysiological recordings were indeed from human neurons differentiated from the nonfluorophore-transduced, iPSC-derived NSCs, biocytin was included in the recording pipette. After recording, the cultures were stained with a streptavadin-labeled secondary antibody to detect biocytin (Figs. 8B, 9C3). We show a biocytin-labeled cell recovered after recording and the immunocytochemistry protocol

labeled with the human cytoplasmic specific marker antibody STEM121 (Fig. 9C1–C4), confirming that the electrophysiologically responsive cell was indeed differentiated from the fibroblast iPSC-derived NSCs. These data show that the NSCs produced with our SB and DMH1 protocol retained their necessary and defining feature, the ability to make functional neurons.

DISCUSSION

Here we describe a rapid, technically easy stem cell culture system that allows for the efficient neural differentiation of PSCs (ePSCs or iPSCs). Adherent, feeder-free, single-cell-passaged PSCs are grown and expanded using a defined medium and then differentiated en masse to NSCs using a completely defined chemical approach. This has allowed us to develop a robust *process-based* approach for deriving populations of NSCs suitable for disease modeling, drug discovery, or transplantation (Table III). We have also defined specific criteria to be used to assess the process at critical junctures as well as to assess the cells in their final state (Table III). Our data demonstrate that the NSCs produced according to this framework are capable of terminal differentiation into functional action-potential-firing neurons as well as glia. The clinical importance of the processes developed so far is that they can be easily adapted to cGMP production (Suppl. Info. Table II) for generation of clinical-grade cells. Stepwise criteria can be applied at each stage of differentiation, including the starting cell culture and its reprogramming; the beginning iPSC culture(s); separation of reprogrammed from non-reprogrammed cells; the final iPSC culture(s) with defined pluripotency and purity; and the final NSC culture defined by specific markers (identity), purity, and safety (absence of undifferentiated iPSCs). For qualification, validation, and potency, the cell products can be tested to determine whether they meet prespecified functional criteria. This would include, for example, demonstration of chemokine receptor expression and chemokine-responsive migration as a measure of the product's ability to migrate within the brain after transplantation and, critically, the ability to mitigate against the targeted disease process. As an example of the latter and using the recently completed phase I trials of bNSCs in Batten's disease (see below) as a case in point, a quantitative in vitro assay demonstrating enzyme cross-correction can be devised.

The process-based approach overcomes the need for many of the PSC culture and neural differentiation steps previously described. For example, feeder cells that support the growth of traditionally cultured PSCs (e.g., ePSCs) can be eliminated. Mouse embryonic fibroblasts (MEFs) are the most commonly used feeder-cell type for coculture with ePSCs; however, the use of MEFs in the production of a transplantable cell population introduces a xenogenic component that necessitates additional characterization and regulatory oversight. The search for nonxenogenic culture systems has led to the use of human-derived feeder cells, extracellular matrix components, and/or growth factors (Ausubel et al., 2011; Bergstrom et al., 2011; Stover and Schwartz, 2011). Importantly, we have adopted defined culture systems that no longer rely on feeder cells for production of the iPSCs and NSCs. Although this eliminates much of the inherent variability of conditioned culture media, it does impose a strict adherence to cell density considerations when passaging, a criterion easily adapted into a process-based approach.

There is a need for reliable and efficient, large-scale expansion of transplantable cell populations. Brain-derived NSCs (bNSCs) have been used for transplantation and neurological repair as well as for disease modeling. Animal studies have shown that bNSCs can integrate into a host brain, providing repair or protection (Gage et al., 1995; Snyder et al., 1995; Svendsen et al., 1999; Brustle et al., 1999; Zhang et al., 2001; Tamaki et al., 2002; Schwartz, 2006; Lee et al., 2007). Importantly, human bNSCs are nontumorigenic and are currently being used in preclinical and phase I clinical trials for a number of diseases. A key step for the successful translational use of human iPSCs is differentiation to a state of NSC identity and purity that is devoid of tumorigenic potential, similar to bNSCs. Although our studies have not been exhaustive in this regard, our data suggest that process-derived NSCs are not tumorigenic and have the capacity to differentiate efficiently into functional neurons. This makes it possible to generate large numbers of PSC-derived neural cells for transplantation (up to at least a 10^{30}-fold expansion), a distinct advantage over bNSCs, whose source and replicative potential are limited.

Another advantage is that neural cells derived from iPSCs can be immune-matched to the recipient, reducing or eliminating the requirement for long-term immunosuppression. Although a report has suggested that iPSCs have an immunogenic potential when transplanted into isogenic hosts, this appears to involve only minor histocompatibility antigens (Zhao et al., 2011). Moreover, the studies were not extended to differentiated derivatives, which are the cells that would actually be transplanted. With our procedure, the major histocompatibility antigens remain unchanged after reprogramming and expansion (Table I), suggesting that immune-matching with iPSC-derived NSCs is still highly likely. This is important isofar as it suggests that the generation of iPSC banks for HLA-matched tissue transplantation based on known donor and recipient HLA types is a worthwhile effort.

All of the required criteria for clinical cell production can easily be incorporated into the backbone process that we have developed. Current FDA guidelines can be incorporated into the process, including donor screening, raw materials sourcing, vendor qualification, process documentation, and assay and process qualification (Carpenter et al., 2009; Csete, 2010). We believe that NSCs derived by this process-type approach are likely to be acceptable to the FDA for INDs proposing patient-specific stem cell therapies (Carpenter et al., 2009; Fink, 2009; Csete, 2010) and, importantly, are not cost prohibitive. The process-based approach does not require a large and expensive dedicated cell production facility (Dietz et al., 2007). Instead, it can be carried out in a single-room facility based on an integrated cell processing work station contained in a class 10000 clean room. This would allow medical centers to offer in-house, patient-specific therapies for the populations with whom they have the most expertise. This will facilitate the movement of iPSC-derived therapies into the clinic.

Supplementary Material

Refer to Web version on PubMed Central for supplementary material.

Acknowledgments

We thank Dr. Randi Hagerman, Michele Ono, Andrew Ligsay, Jonathan Polussa, and Lily Ngotran of the UCDavis MIND Institute for the patient recruitment and biopsy accrual. We also thank Brian Fury, UC Davis, for helpful advice on $CD34^+$ HSC propagation and Dr. Flora Tassone for analysis of FXS-derived specimens. We thank Dr. Nabuko Uchida of StemCells, Inc., for the kind gift of the human-specific cytoplasmic antigen antibody STEM121. We gratefully acknowledge the Children's Miracle Network for the gift of the Eppendorf Femtojet. We are also grateful to Dr. Leonard Sender and the staff of the CHOC BMT Lab/Cord Blood Bank for the samples of umbilical cord blood used for our CD34+ cell isolations. We especially thank Dr. Mei Chang for the flow cytometry acquisition and Betty Sicaeros for help with glial cell culture preparation. The NCI Preclinical Repository generously supplied FGF-2.

Contract grant sponsor: National Institutes of Health; Contract grant number: T15HL074286 (to P.H.S.); Contract grant number: R01HD059967 (to P.H.S.; appropriately using only ePSC lines on the NIH hESC Repository at the time the grant that was being used for funds was in force); Contract grant sponsor: Autism Speaks (to P.H.S., D.K.O.); Contract grant sponsor: California Institute for Regenerative Medicine; Contract grant number: TR3-05476 (to P.H.S.); Contract grant sponsor: Human Neural Stem Cell Resource.

References

Ausubel LJ, Lopez PM, Couture LA. GMP scale-up and banking of pluripotent stem cells for cellular therapy applications. Methods Mol Biol. 2011; 767:147–159. [PubMed: 21822873]

Bajpai R, Lesperance J, Kim M, Terskikh AV. Efficient propagation of single cells Accutase-dissociated human embryonic stem cells. Mol Reprod Dev. 2008; 75:818–827. [PubMed: 18157870]

Belmonte JC, Ellis J, Hochedlinger K, Yamanaka S. Induced pluripotent stem cells and reprogramming: seeing the science through the hype. Nat Rev Genet. 2009; 10:878–883. [PubMed: 19859062]

Bergstrom R, Strom S, Holm F, Feki A, Hovatta O. Xeno-free culture of human pluripotent stem cells. Methods Mol Biol. 2011; 767:125–136. [PubMed: 21822871]

Brennand KJ, Simone A, Jou J, Gelboin-Burkhart C, Tran N, Sangar S, Li Y, Mu Y, Chen G, Yu D, McCarthy S, Sebat J, Gage FH. Modelling schizophrenia using human induced pluripotent stem cells. Nature. 2011; 473:221–225. [PubMed: 21490598]

Brustle O, Jones KN, Learish RD, Karram K, Choudhary K, Wiestler OD, Duncan ID, McKay RD. Embryonic stem cell-derived glial precursors: a source of myelinating transplants. Science. 1999; 285:754–756. [PubMed: 10427001]

Carpenter MK, Frey-Vasconcells J, Rao MS. Developing safe therapies from human pluripotent stem cells. Nat Biotechnol. 2009; 27:606–613. [PubMed: 19587662]

Chambers SM, Fasano CA, Papapetrou EP, Tomishima M, Sadelain M, Studer L. Highly efficient neural conversion of human ES and iPS cells by dual inhibition of SMAD signaling. Nat Biotechnol. 2009; 27:275–280. [PubMed: 19252484]

Csete M. Translational prospects for human induced pluripotent stem cells. Regen Med. 2010; 5:509–519. [PubMed: 20632855]

Dietz AB, Padley DJ, Gastineau DA. Infrastructure development for human cell therapy translation. Clin Pharmacol Ther. 2007; 82:320–324. [PubMed: 17637785]

Fink DW Jr. FDA regulation of stem cell-based products. Science. 2009; 324:1662–1663. [PubMed: 19556496]

Gage FH, Coates PW, Palmer TD, Kuhn HG, Fisher LJ, Suhonen JO, Peterson DA, Suhr ST, Ray J. Survival and differentiation of adult neuronal progenitor cells transplanted to the adult brain. Proc Natl Acad Sci U S A. 1995; 92:11879–11883. [PubMed: 8524867]

Gonzalez R, Lee JW, Snyder EY, Schultz PG. Dorsomorphin promotes human embryonic stem cell self-renewal. Angew Chem Int Ed Engl. 2011; 50:3439–3441. [PubMed: 21384475]

Hao J, Ho JN, Lewis JA, Karim KA, Daniels RN, Gentry PR, Hopkins CR, Lindsley CW, Hong CC. In vivo structure–activity relationship study of dorsomorphin analogues identifies selective VEGF and BMP inhibitors. ACS Chem Biol. 2010; 5:245–253. [PubMed: 20020776]

Hilgenberg LG, Ho KD, Lee D, O'Dowd DK, Smith MA. Agrin regulates neuronal responses to excitatory neurotransmitters in vitro and in vivo. Mol Cell Neurosci. 2002; 19:97–110. [PubMed: 11817901]

Kambal A, Mitchell G, Cary W, Gruenloh W, Jung Y, Kalomoiris S, Nacey C, McGee J, Lindsey M, Fury B, Bauer G, Nolta JA, Anderson JS. Generation of HIV-1 resistant and functional macrophages from hematopoietic stem cell-derived induced pluripotent stem cells. Mol Ther. 2011; 19:584–593. [PubMed: 21119622]

Lee JP, Jeyakumar M, Gonzalez R, Takahashi H, Lee PJ, Baek RC, Clark D, Rose H, Fu G, Clarke J, McKercher S, Meerloo J, Muller FJ, Park KI, Butters TD, Dwek RA, Schwartz P, Tong G, Wenger D, Lipton SA, Seyfried TN, Platt FM, Snyder EY. Stem cells act through multiple mechanisms to benefit mice with neurodegenerative metabolic disease. Nat Med. 2007; 13:439–447. [PubMed: 17351625]

Morizane A, Doi D, Kikuchi T, Nishimura K, Takahashi J. Small-molecule inhibitors of bone morphogenic protein and activin/nodal signals promote highly efficient neural induction from human pluripotent stem cells. J Neurosci Res. 2011; 89:117–126. [PubMed: 21162120]

Muotri AR, Nakashima K, Toni N, Sandler VM, Gage FH. Development of functional human embryonic stem cell-derived neurons in mouse brain. Proc Natl Acad Sci U S A. 2005; 102:18644–18648. [PubMed: 16352714]

Neely MD, Litt MJ, Tidball AM, Li GG, Aboud AA, Hopkins CR, Chamberlin R, Hong CC, Ess KC, Bowman AB. DMH1, a highly selective small molecule BMP inhibitor promotes neurogenesis of hiPSCs: comparison of PAX6 and SOX1 expression during neural induction. ACS Chem Neurosci. 2012; 3:482–491. [PubMed: 22860217]

Nethercott HE, Brick DJ, Schwartz PH. Immunocytochemical analysis of human pluripotent stem cells. Methods Mol Biol. 2011; 767:201–220. [PubMed: 21822877]

Pankratz MT, Li XJ, Lavaute TM, Lyons EA, Chen X, Zhang SC. Directed neural differentiation of human embryonic stem cells via an obligated primitive anterior stage. Stem Cells. 2007; 25:1511–1520. [PubMed: 17332508]

Robinson J, Waller MJ, Fail SC, McWilliam H, Lopez R, Parham P, Marsh SG. The IMGT/HLA database. Nucleic Acids Res. 2009; 37:D1013–D1017. [PubMed: 18838392]

Schwartz PH. The potential of stem cell therapies for neurological diseases. Expert Rev Neurother. 2006; 6:153–161. [PubMed: 16466295]

Schwartz PH, Bryant PJ, Fuja TJ, Su H, O'Dowd DK, Klassen H. Isolation and characterization of neural progenitor cells from post-mortem human cortex. J Neurosci Res. 2003; 74:838–851. [PubMed: 14648588]

Schwartz PH, Brick DJ, Stover AE, Loring JF, Muller FJ. Differentiation of neural lineage cells from human pluripotent stem cells. Methods. 2008; 45:142–158. [PubMed: 18593611]

Schwartz PH, Brick DJ, Nethercott HE, Stover AE. Traditional human embryonic stem cell culture. Methods Mol Biol. 2011; 767:107–123. [PubMed: 21822870]

Snyder EY, Taylor RM, Wolfe JH. Neural progenitor cell engraftment corrects lysosomal storage throughout the MPS VII mouse brain. Nature. 1995; 374:367–370. [PubMed: 7885477]

Stover AE, Schwartz PH. Adaptation of human pluripotent stem cells to feeder-free conditions in chemically defined medium with enzymatic single-cell passaging. Methods Mol Biol. 2011; 767:137–146. [PubMed: 21822872]

Svendsen CN, Caldwell MA, Ostenfeld T. Human neural stem cells: isolation, expansion and transplantation. Brain Pathol. 1999; 9:499–513. [PubMed: 10416990]

Takahashi K, Tanabe K, Ohnuki M, Narita M, Ichisaka T, Tomoda K, Yamanaka S. Induction of pluripotent stem cells from adult human fibroblasts by defined factors. Cell. 2007; 131:861–872. [PubMed: 18035408]

Tamaki S, Eckert K, He D, Sutton R, Doshe M, Jain G, Tushinski R, Reitsma M, Harris B, Tsukamoto A, Gage F, Weissman I, Uchida N. Engraftment of sorted/expanded human central nervous system stem cells from fetal brain. J Neurosci Res. 2002; 69:976–986. [PubMed: 12205691]

Watanabe K, Ueno M, Kamiya D, Nishiyama A, Matsumura M, Wataya T, Takahashi JB, Nishikawa S, Nishikawa S, Muguruma K, Sasai Y. A ROCK inhibitor permits survival of dissociated human embryonic stem cells. Nat Biotechnol. 2007; 25:681–686. [PubMed: 17529971]

Yu J, Vodyanik MA, Smuga-Otto K, ntosiewicz-Bourget J, Frane JL, Tian S, Nie J, Jonsdottir GA, Ruotti V, Stewart R, Slukvin II, Thomson JA. Induced pluripotent stem cell lines derived from human somatic cells. Science. 2007; 318:1917–1920. [PubMed: 18029452]

Zhang SC, Wernig M, Duncan ID, Brustle O, Thomson JA. In vitro differentiation of transplantable neural precursors from human embryonic stem cells. Nat Biotechnol. 2001; 19:1129–1133. [PubMed: 11731781]

Zhao T, Zhang ZN, Rong Z, Xu Y. Immunogenicity of induced pluripotent stem cells. Nature. 2011; 474:212–215. [PubMed: 21572395]

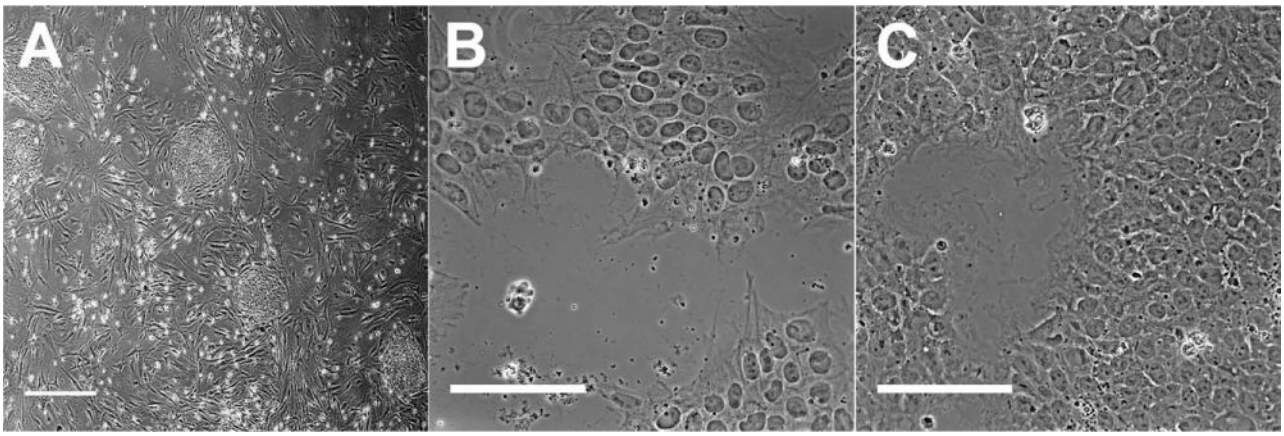

Fig. 1.

Phase-contrast comparison of classical PSC culture on MEFs with single-cell Accutase passaging and StemPro culture. **A:** PSCs (WA01.1-EI26-000.M8) mechanically passaged and transferred onto a feeder layer of irradiated MEFs showing classical PSC colony formation. ×4. **B,C:** Despite being seeded as single cells, Accutase-passaged cells quickly migrate to form small colonies with a great deal of obvious membranous material (Supp. Info. Video 1). B shows an early time (about 16 hr) after plating of PSCs (BG01.1-EI27-000.M6S6) continually passaged (six times) using Accutase and StemPro. ×40. C shows a later time (about 40 hr) after plating of PSCs (WA09.1-EI26-000.M8S16) continually passaged (16 times) using Accutase and StemPro. ×40. Scale bars = 500μm in A; 50 μm in B,C.

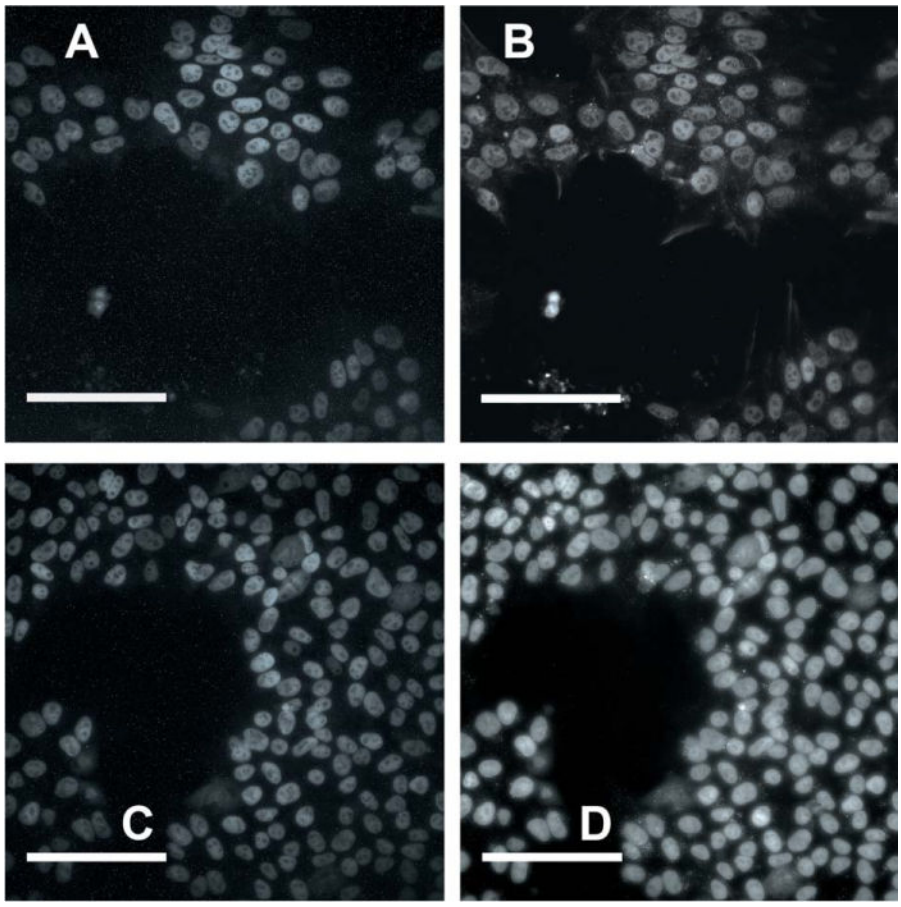

Fig. 2.

Immunofluorescence staining of StemPro/Accutase/Matrigel-grown PSC cultures showing maintenance of pluripotency markers. BG01.1-EI27-000.M6S6 (**A,B** and WA09.1-EI26-000.M8S16 (**C,D** PSC cultures that were originally grown on MEFs and were transitioned to StemPro cultures with Accutase passaging. Cells were stained with a mouse monoclonal antibody to Oct-4 (A,C) or a goat polyclonal antibody to Sox-2 (B,D). ×40. Scale bars = 50μm. [Color figure can be viewed in the online issue, which is available at wileyonlinelibrary.com.]

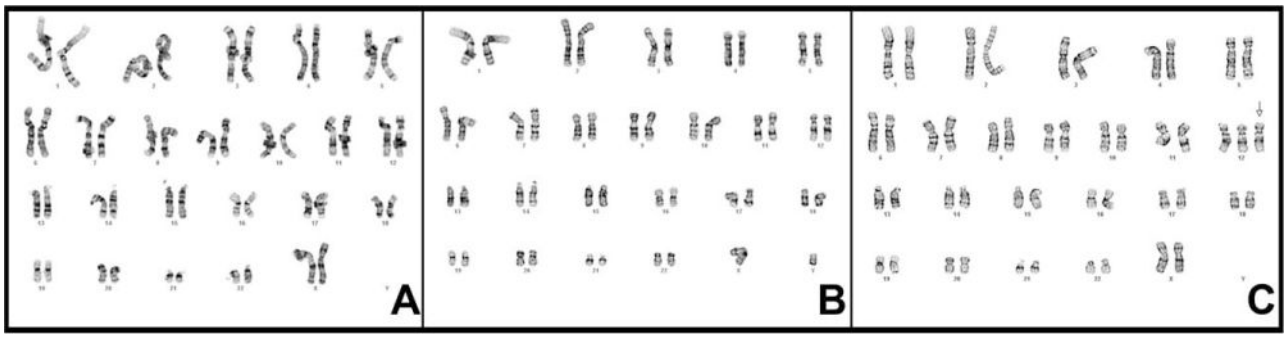

Fig. 3.

Chromosome spreads of Accutase-passaged StemPro PSC cultures. **A:** BG03.1-EI26-000.M2S20[46,XX], 20 StemPro passages without ROCK inhibitor. **B:** BG01.1-EI27-000.M6S20[46,XY], from S16 with ROCK inhibitor. **C:** WA09.1-EI26-000.M8S40[47,XX,+12], 40 StemPro passages without ROCK inhibitor.

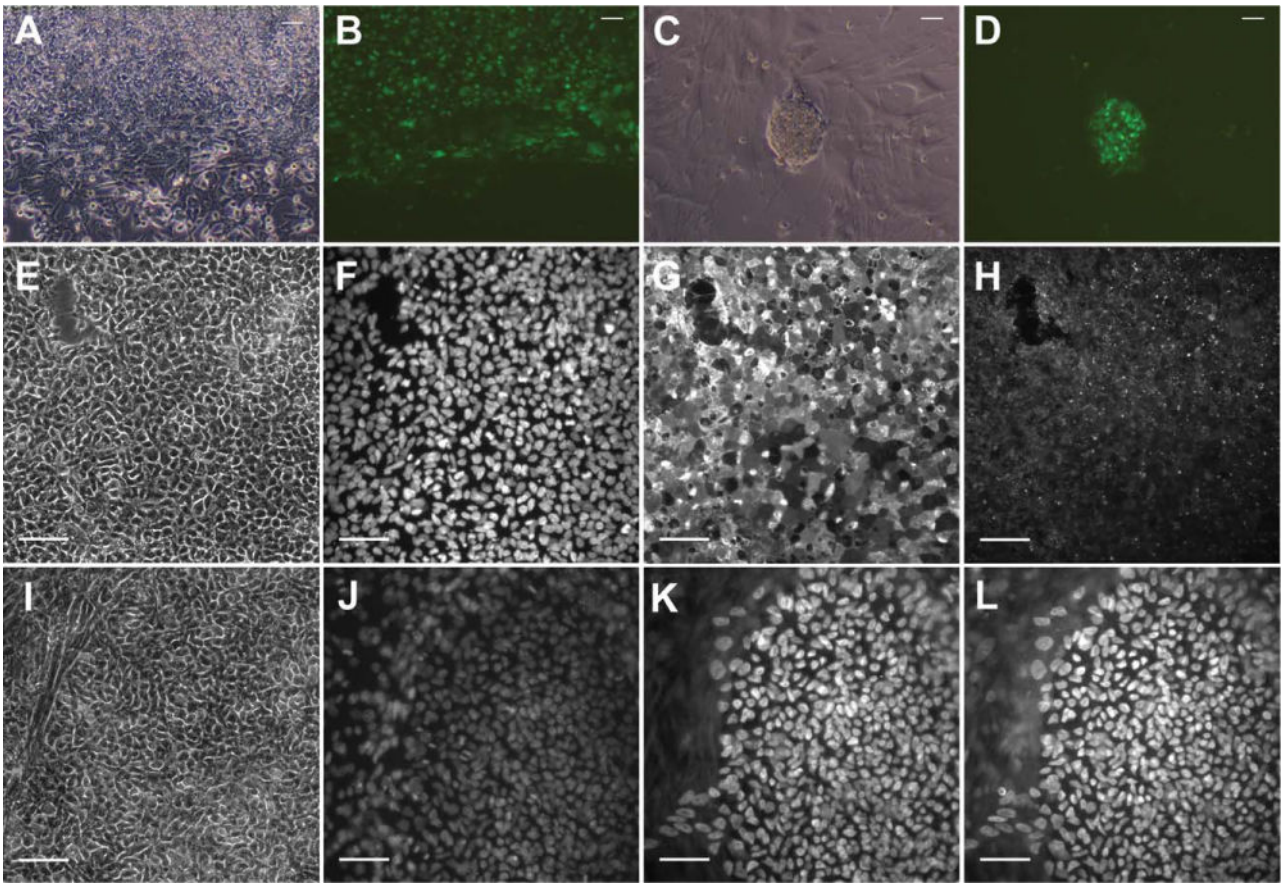

Fig. 4.

Staining of lentivirus- and Sendai virus-derived iPSCs from control and ASD cells. Clonal colonies with PSC morphology that stained strongly positive for Tra-1–60 (live staining) were picked for expansion, and colonies that showed the best morphology and homogeneity of staining with the PSC markers Nanog and Oct-4 were continuously expanded in culture. Phase-contrast images (**A,C,E,I**), DAPI staining (**F,J**), live Tra1–60 immunofluorescence (**B,D**), and immunocytochemical staining for Tra-1–60 (**G**), SSEA-4 (**H**), Nanog (**K**), and Sox-2 (**L** of SV-derived SC151.7-SF4-2I4.M5 iPSCs (A,B), LV-derived SC110.4-SF7-1I2.M8 iPSCs (C,D), LV-derived SC27.1-BN10-1I2.M4 iPSCs (E–H), and LV-derived SC30.1-BN10-1I3.M2 iPSCs (I–L) cultures. Scale bars = 50μm.

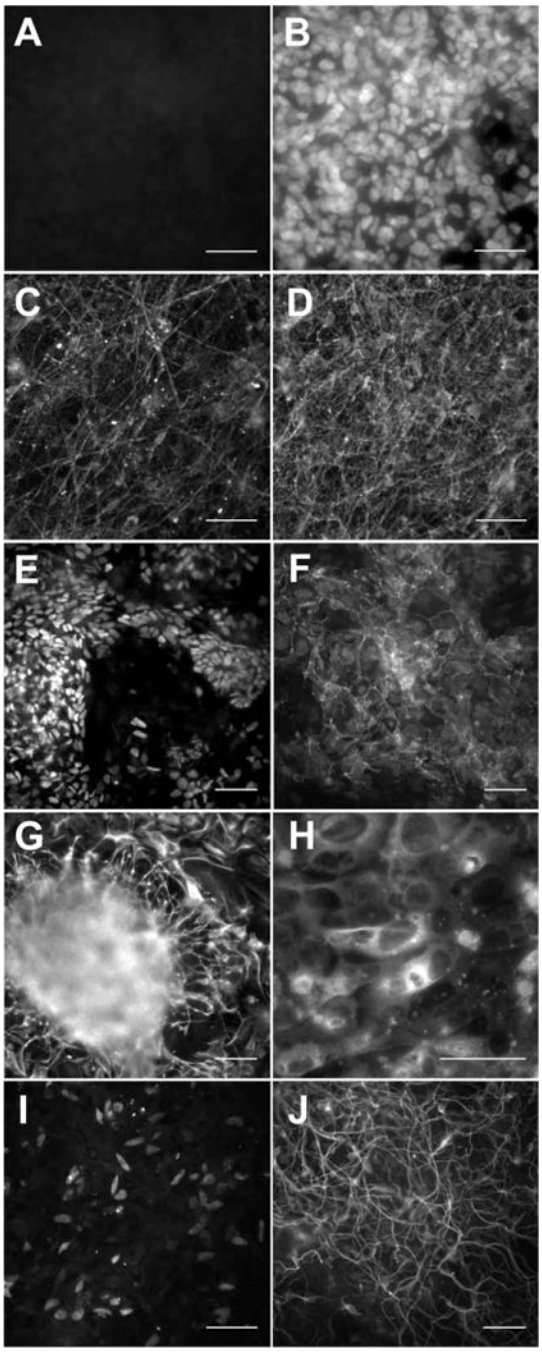

Fig. 5.

Efficient, feeder-free, adherent-cell, defined differentiation of human ePSC and iPSC cultures to NSCs. NSC-differentiating ePSCs (BG03.1-EI26-000.M2S20-N1 [**C–G,I,J**]) and iPSCs (SC101.7-SF4-1I3.M10S5-N7 [**A,B**] and SC105.9-SF4-1I6.M24S5-N2 [**H**]) were characterized by immunofluorescence microscopy for the following markers: A, Oct-4; B, Pax-6; C, Forse-1; D, NCAM; E, Sox-1; F, N-CAD; G, nestin; H, CXCR-4; I, Olig-2; and J, β-tubulin. Scale bars = 50μm.

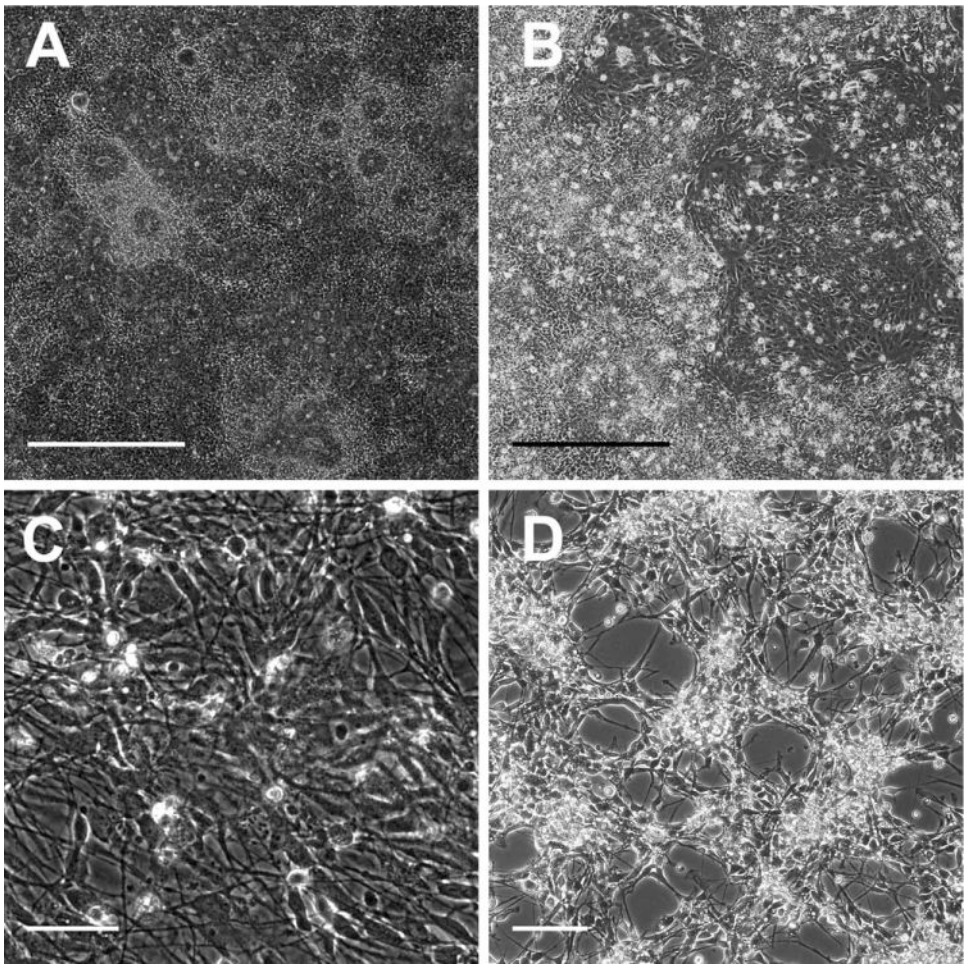

Fig. 6.

Efficient, defined, chemical NSC induction from adherent, defined StemPro-adapted iPSC and ePSC cultures. Phase-contrast images showing the classical neural rosette morphology of NSCs derived from Accutase-passaged StemPro cultures of SC30.1-BN10-1I3.M2S4-N1 iPSCs (**A** following directed differentiation with Noggin and SB. ×10. WA09.1-EI26-000.M8S22-N2 ePSCs (**B** following directed differentiation with DMH1 and SB. ×10. BG03.1-EI26-000.M2S20-N2 ePSCs (**C** following directed differentiation with DMH1 and SB at higher magnification (×60) to show the resemblance to classical human brain-derived NSC cultures SC27.1-BN10 (Schwartz et al., 2003) as shown in **D**. ×40. Scale bars = 500μm in A,B; 50μm in C,D.

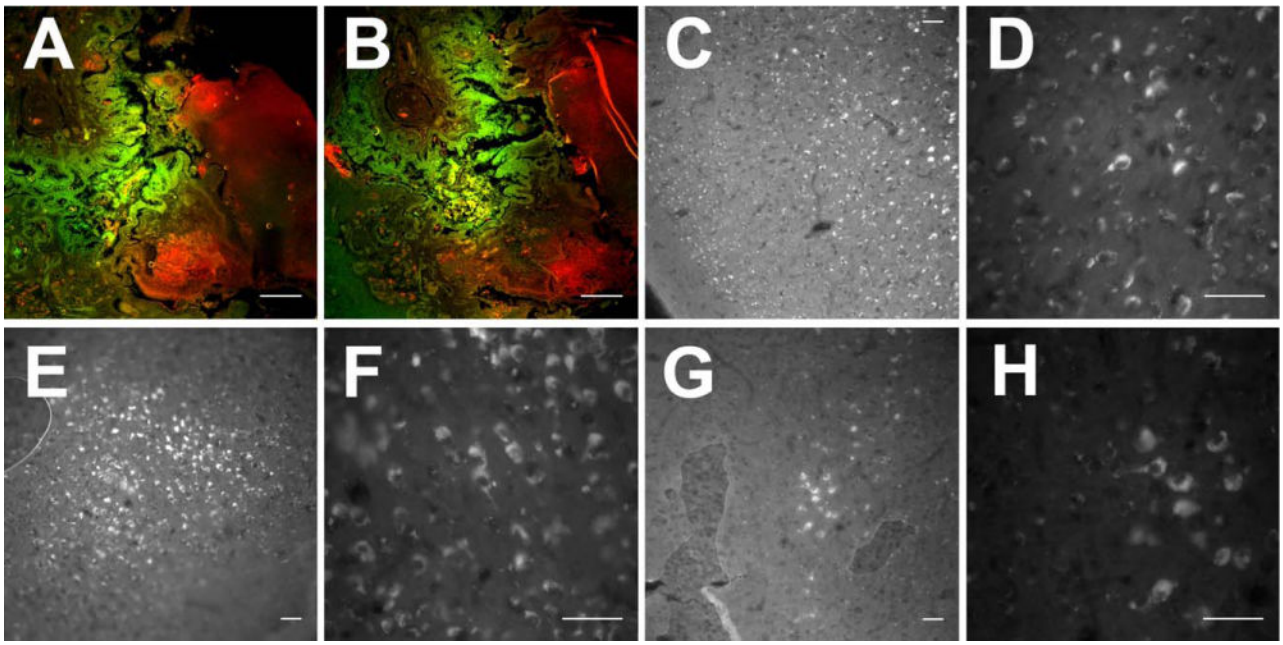

Fig. 7.

Distribution of GFP- and/or mCherry-labeled cells after intracerebroventricular PSC injection [WA01.1-EI26-000.M32S21(mCh1), WA01.1-EI26-000.M32S21(GFP1); **A,B**] or NSC injection [WA01.1-EI26-000.M32S21(GFP1)-N7; **C–H**] in NSG mice. PSCs formed tumors in all cases examined. The tumors were almost always segregated by fluorophore (A,B; ×4), suggesting clonal expansion of only some of the injected cells. By contrast, PSC-derived NSCs never formed tumors or multicellular aggregates and appeared as single cells relatively evenly distributed in a variety of brain structures. C,D, E,F, and G,H show paired ×20 and ×60 images of frontal cortex, basal ganglia, and parietal cortex, respectively. Apical neurites can clearly be seen on some cells, suggesting neuronal differentiation. Scale bars = 500μm in A,B; 50μm in C–H.

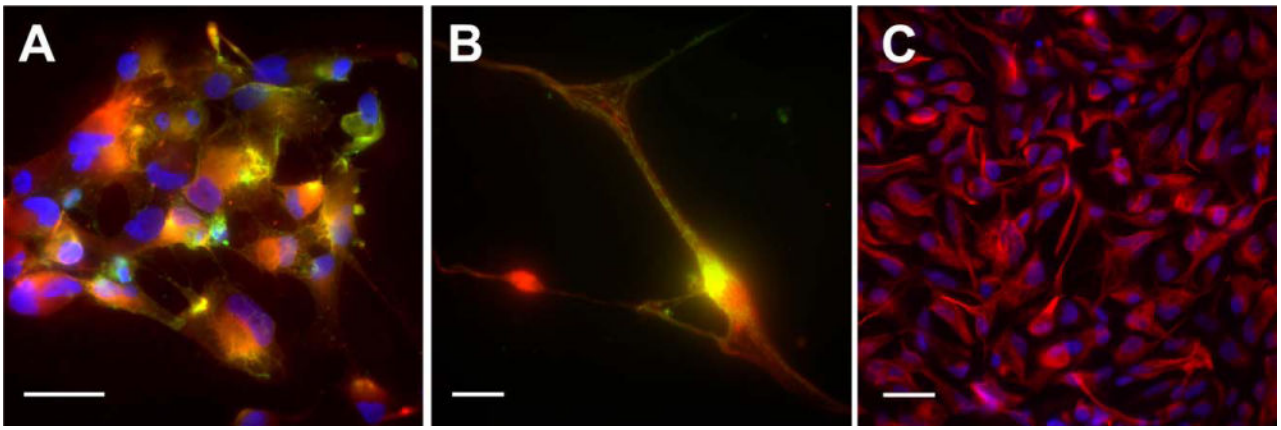

Fig. 8.

Process derived-NSCs can be terminally differentiated to neurons and glia. Immunofluorescence analysis of completely defined, small-molecule (DMH1 and SB)-directed NSC cultures that were either terminally differentiated to neurons (SC122.6-SF4-1I1M20S13-N2G8-3Nn80 [**A**], SC122.6-SF4-1I1M20S13-N2G12-4Nn60 [**B**]) in coculture with rat (A) or mouse (B) glia or terminally differentiated to astrocytes (SC171.7-SF5-1I1M6S12-N2G5-5A100; **C**). A is a composite image showing expression of the terminal neuronal markers synapsin (green) and MAP2ab (red) with nuclear counterstaining by DAPI (blue). B shows expression of the postsynaptic marker PSD-95 (red) on a biocytin (green)-injected neuron (this cell was subjected to electrophysiological recording as described in Fig. 9). C shows expression of the astrocyte-specific marker S100β (red) with nuclear counterstaining by DAPI (green). Scale bars = 50 μm.

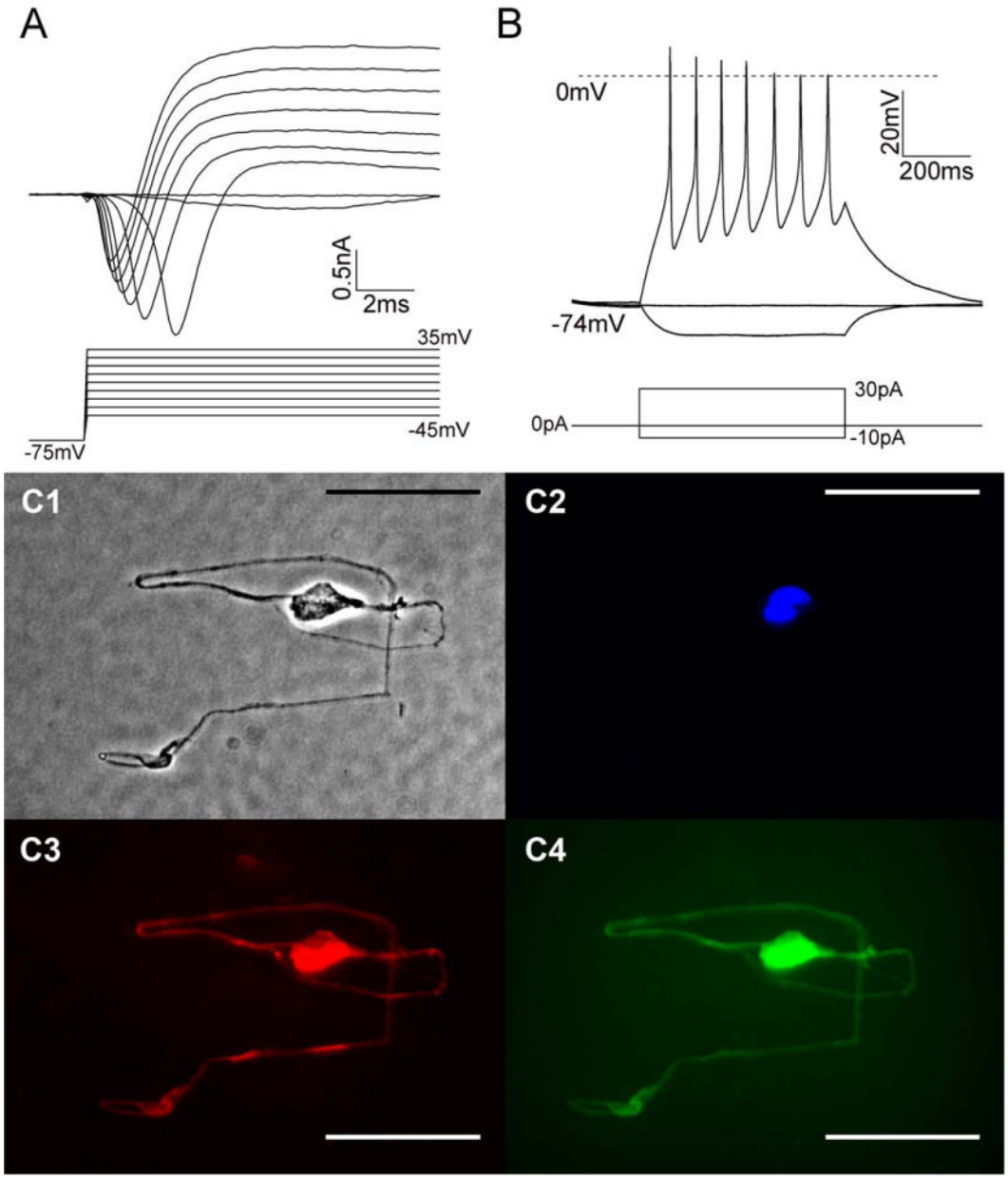

Fig. 9.

Process-derived NSCs yield functional neurons. **A:** Whole-cell voltage-clamp recording of a neuron derived from one line (SC122.6-SF4-1I1M20S13-N2G12-4Nn60) reveals a composite current with both inward sodium and outward potassium components in a neuron differentiated from human iPSC-derived NSCs. **B:** Current-clamp recording from the same neuron demonstrating the ability to fire multiple, overshooting action potentials in response to depolarizing current injection. **C:** Immunofluorescence analysis demonstrating that another recorded neuron filled with biocytin during whole-cell recording colabeled with the human-specific marker STEM121. C1: Phase-contrast image of recorded neuron. C2: Nuclear counterstaining with DAPI (blue). C3: Biocytin detection using a streptavidin-

labeled fluorophore (red). C4: Colabeling of the biocytin-filled, electrically active neuron with the human-specific marker STEM121 (green).

TABLE I

HLA Typing Comparison of Sendai Virus iPSCs Derived From CD34$^+$ HSCs With the Identical CD34$^+$ HSCs Used as the Reprogramming Starting Material[a]

	A locus		B locus		C locus		DRB1 locus		DQA1 locus		DQB1 locus		DPB1 locus	
ID	**Allele 1**	**Allele 2**	**Allele 1**	**Allele 2**	**Allele 1**	**Allele 2**	**Allele 1**	**Allele 2**	**Allele 1**	**Allele 2**	**Allele 1**	**Allele 2**	**Allele 1**	**Allele 2**
SC53.1-UH1	2.03	29.02	38.02	51.01	07.02	15.09	14.06	15.02	01.01	5.03	3.01	5.01	4.01	13.01
SC53.1-UH1–2I1.M5S10	2.03	29.02	38.02	51.01	07.02	15.09	14.06	15.02	01.01	5.03	3.01	5.01	4.01	13.01

[a]Total DNA was isolated from either iPSCs or CD34$^+$ HSCs using the Qiagen DNeasy Blood and Tissue Kit. HLA typing was performed by HLA Lab Services of Life Technologies. This screen accounts for more than 96% of existing HLA types and shows that the HLA type is stable under our reprogramming and culture conditions.

TABLE II

ICC/Flow Cytometry Comparison of PSCs (ePSCs and iPSCs) With Skin Fibroblasts and PSC-Derived NSCs[a]

Antibody marker	Fibroblasts	PSCs	NSCs
Sox-1	+	+	+++
Nanog[b]	ND	+++	−
Oct-4[b]	−	+++	−
Sox-2	−	+++	+++
Tra-1–60[b]	−	+++	−
PAX-6[c]	−	−	+++
Forse-1	−	+	+++
Nestin	+	+	+++
N-CAD	−	−/+	++
N-CAM	ND	−/+	+++
Tbr-2	+	++	+++
Olig-2	ND	−	++
CXCR4	−	−/+	+++
β-tubulin	ND	−	++

[a] +, light staining; ++, moderate staining; +++, strong staining; −, undetectable staining; ND, not determined.

[b] Discriminating markers between PSCs and NSCs.

[c] Best discriminating markers between PSCs and NSCs.

TABLE III

Qualitative and Quantitative Criteria Used for Assessment of Cells as They Progress Through the Process That Changes Them From Source Material to Transplantable Cells (or Cells Useful for Drug Discovery or Disease Modeling)[a]

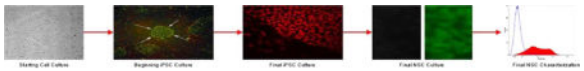

Phenotype	e.g., Fibroblasts/ HSCs	Beginning iPSCs	Final iPSCs	Final NSCs	Functionality
Nomenclature	SC200.1-SF4	SC200.1-SF4-1I1.M1	SC200.1-SF4-1I1.M20S20	SC200.-SF4-1I1.M20S20-N2G4	SC200.-SF4-1I1.M20S20-N2G4
Morphology	Fibroblastic	Small colony of small cells	Medium to large colonies of small cells with high nucleus-to-cytoplasm ratios and prominent nucleoli	Elongated cells. No visible colonies of PSC morphology	–
Pathogenicity	Donor blood screen negative	–	–	Negative for gram +/− bacteria, mycoplasma, fungi	–
Live Staining	–	Tra-1–60 positive	–	–	–
ICC	–	–	>95% Nanog, Oct4 positive	>95% Pax6, Sox2, Sox1, nestin positive; Oct4, Nanog negative	–
RT-PCR	–	–	Bright bands for Oct 4, Sox2, Nanog, Cripto	Bright bands for Pax6, Sox2, Sox1, nestin positive; Oct4, Nanog negative	–
Flow Cytometry	–	–	>95% Tra-1–60, SSEA4 positive	Tra-1–60, SSEA4 negative, >90% CXCR4 bright	–
Migration	–	–	–	–	>90% Migrate to SDF1α
Disease-specific functionality	–	–	–	–	Enzyme cross-correction to enzyme-negative cells

[a]The nomenclature ensures accurate identification of cellular phenotypes throughout the process.